JOURNAL OF THE ROYAL SOCIETY Interface

CrossMark click for updates

J. R. Soc. Interface (2012) **9**, 2299–2308
doi:10.1098/rsif.2011.0887
Published online 2 May 2012

Structure and physical properties of silkworm cocoons

Fujia Chen*, David Porter and Fritz Vollrath

Department of Zoology, University of Oxford, South Parks Road, OX1 3PS, UK

Silkworm cocoons have evolved a wide range of different structures and combinations of physical and chemical properties in order to cope with different threats and environmental conditions. We present our observations and measurements on 25 diverse types of cocoons in a first attempt to correlate physical properties with the structure and morphology of the cocoons. These two architectural parameters appear to be far more important than the material properties of the silk fibres themselves. We consider tensile and compressive mechanical properties and gas permeation of the cocoon walls, and in each case identify mechanisms or models that relate these properties to cocoon structure, usually based upon non-woven fibre composites. These properties are of relevance also for synthetic non-woven composite materials and our studies will help formulate bio-inspired design principles for new materials.

Keywords: silk; cocoon; mechanical properties; permeability; non-woven; biomimetic

1. INTRODUCTION

Silk materials have received much attention in recent years because of their attractive combinations of mechanical strength and toughness as well as the environmentally benign conditions under which the materials are processed from concentrated protein solutions to solid fibres [1]. However, silkworm cocoons, which are best known as the main commercial source of silk material (primarily for textiles), are themselves remarkable natural composite materials. While the commercial silkworm *Bombyx mori* has been cultivated by man for about five thousand years, a wide range of wild silkworms have evolved independently over the world over hundreds of thousands of years, and each has a slightly different combination of morphology and properties that have adapted to cope with diverse local environments.

A cocoon is a natural silk composite with a non-woven structure made of continuous silk fibres conglutinated by sericin bonding matrix. As a biological structural material, it has a hierarchical structure that we assume has been optimized through evolutionary pressures over millions of years to provide the optimum protection for the silkworm pupae as they transform into moths, and are exposed to a wide range of threats such as physical attack from animals, birds or insects, or more subtle threats such as bacteria or simply harsh environmental conditions. The key point here is that they are all, in themselves, optimized for function and that we should be able to learn from this wide range of optimized structure–property–function relations in cocoons. Figure 1 shows a hierarchical set of pictures of the *B. mori* cocoon structure, from the full cocoon to the individual fibre–sericin combination. These cocoons have been cultivated for yield and ease of reeling of the silk fibres and for their whiteness in textiles, so their morphology is an open non-woven form that can be unwound relatively easily after soaking in mild degumming agents.

Ecologists have suggested that wild silkworm cocoons have evolved (i) for protection against diverse threats and also (ii) to regulate the environment such as to help conserving/blocking water or regulating the flow of gasses such as oxygen and carbon dioxide for the pupae as they develop [2,3]. In order to test these hypotheses, a limited amount of research has been conducted recently to investigate the mechanical properties and gas diffusability of silk cocoons from *B. mori* and *Hyalophora cecropia*. For example, Zhao *et al.* tested the tensile properties of *B. mori* cocoons and found them anisotropic with graded-layer properties [4,5]. The *H. cecropia* cocoons and fibres have also been measured by Reddy *et al.* [6]. Blossman-Myer *et al.* [7] have found that *B. mori* cocoon did not obstruct the exchange of respiratory gases between the pupa and the environment.

In a focused study of three specific cocoon types with a non-woven fibre composite structure, we have previously shown that a quantitative understanding of the mechanism for their tensile mechanical properties offers a novel design route for a remarkably wide range of fibre and particulate composite materials, from paper and nanofibre mats to concrete and polymer-bonded explosives [8]. Here, we extend our study of silkworm cocoons to the much wider range of highly diverse cocoon types from 25 different silkworm species comprising a broad range of morphologies and physical properties. We also discuss how the different structures might control natural tensile,

*Author for correspondence (fujia.chen@zoo.ox.ac.uk).

Electronic supplementary material is available at http://dx.doi.org/10.1098/rsif.2011.0887 or via http://rsif.royalsocietypublishing.org.

Received 17 December 2011
Accepted 17 February 2012

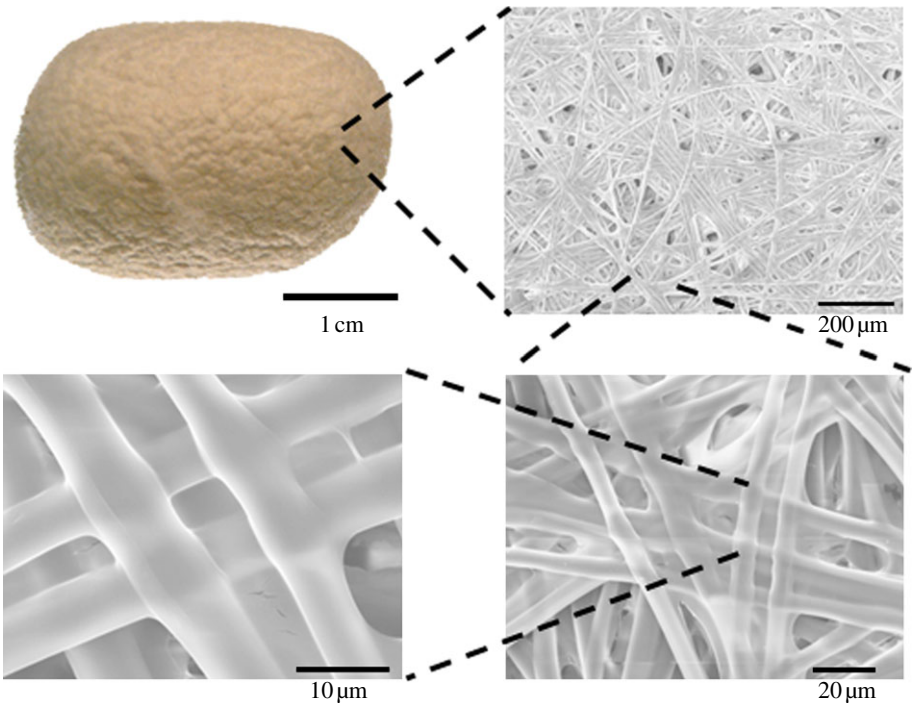

Figure 1. The hierarchy of the morphology of a *Bombyx mori* cocoon. (Online version in colour.)

compressive and gas diffusion properties. We believe this study will be the basis for further biomimetic studies into the design and manufacture of artificial fibre composites with novel morphologies and associated material properties. After all, these are the same key properties that are important in both standard non-woven fibre composites and other materials for engineering applications [9–14]. Cocoon materials have evolved and been optimized in their property combinations and have a wide range of different morphologies with similar silk.

2. RESULTS AND DISCUSSION

2.1. Morphology

As the first step in this investigation of structure–property–function relations in silkworm cocoons, we simply analysed the composition and morphology of 25 different cocoon types reported elsewhere [15]. Scanning electron microscopy (SEM) analysis of the outer surfaces of the silkworm cocoons illustrates the wide range of structures evolved by a moth in Lepidoptera of important silk producing order (figure 2). At the most general level, all of the cocoons have a connected and porous fibre structure. While cocoons like *B. mori* have a highly porous non-woven structure, other cocoons like *Saturnia pyri* and *Actias luna* have very low porosity with the fibres densely packed and bonded by an almost continuous film of sericin. Some of the cocoons have a lattice structure with large fabricated holes with sizes up to 5 mm, e.g. *Caligula simla* and *Caligula cachara*. There are also cocoons combining both non-woven fibre structure and a fibre mesh structure with large holes, e.g. *Cricula trifenestrata* and *Argema mimosae*.

Cocoons could have either a multiple-layer or a single-layer structure. Here, we would like to define a layer in a cocoon as a two-dimensional fibre arrangement with few fibre connections or interweaving to other adjacent two-dimensional fibre arrangements. Most of the cocoons examined by us have multiple layers parallel to the surface direction with sericin bonds between them. The interlayer bonding could be either strong with only little space between layers (e.g. *S. pyri*, *Opodiphtheara eucalypti*), or relatively weak to form a three-dimensional non-woven structure in the cocoon (e.g. *B. mori, Antheraea pernyi*). The cocoon of *Antheraea roylei* has a double cocoon structure with a large and irregular outer 'bag' enclosing an inner cocoon shell without any connections. At the other extreme, some of the cocoons have only a single layer, e.g. *Actias* and *Cricula* cocoons.

Calcium oxalate crystals can be found on some of the cocoon surfaces [16], and this feature may have a functional role. The side lengths of a crystal vary from 1 to 30 µm with the crystals being attached to the fibres and filling the gaps between then, thereby decreasing cocoon porosity. In the *A. roylei* cocoon, only the inner cocoon shell has crystals on its surface. The wider function of calcium oxalate has not yet been investigated in detail and this trait of many cocoons is hence still little understood.

Every one of the cocoons discussed here has a different combination of morphological features and hence also different combinations of mechanical and diffusion properties. It is this diversity of optimized forms that we investigate here for guides to mechanisms that control properties, which can then be exploited by biomimetic synthetic analogues.

2.2. Fibre properties

Silk fibres that are spun into cocoons are in the form of a bave, i.e. a pair of fibroin brins with a sericin covering. This wet or moist covering binds the fibres

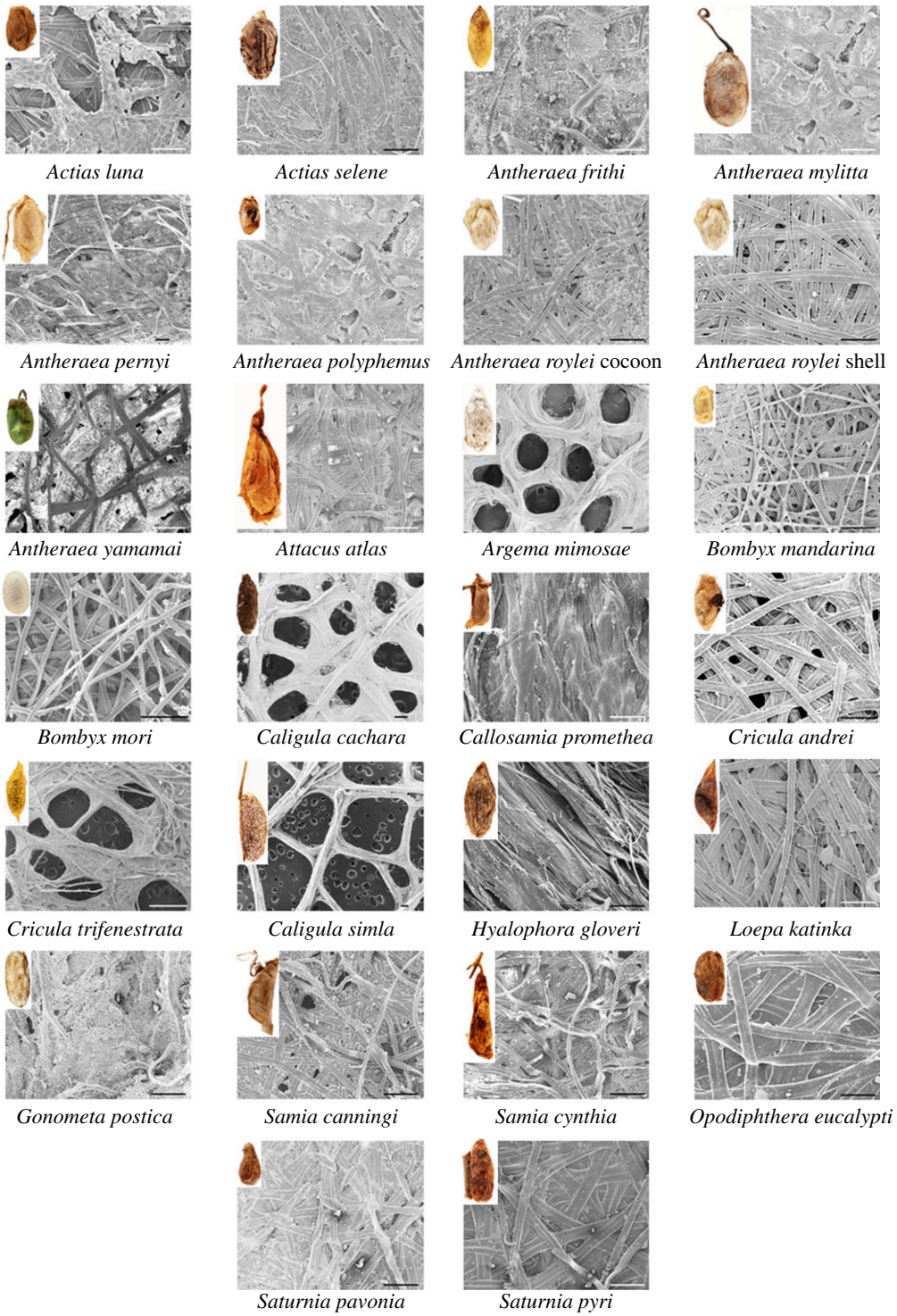

Figure 2. Morphology of silkworm cocoons. Inset: photos of silkworm cocoons. Scale bars: 200 μm.

together and acts as the non-woven composite matrix phase for the cocoon. We tested for reference non-degummed fibres with intact sericin coatings unravelled from cocoons in order to examine whether inherent fibre brin properties may play a statistically significant role in cocoon properties. Figure 3*b* shows that the fibre strength has little correlation ($R^2 = 0.2$) with cocoon strength, which is typical of the poor correlation between fibre and cocoon properties. Otherwise, figure 3*a* shows a few characteristic average stress–strain curves for a number of silk types. All the fibres share a similar initial modulus and a yield at 2–4% strain. Importantly, most fibres have a strain at break around 16 per cent. Initial inspection of the data may give the impression of high variability between silk types, but a comparable plot for a single silk type, a *S. pyri* fibre, demonstrates comparable sample variability (figure 3*c*). We find that samples taken from different layers in cocoons differ significantly, and even spatially close samples can be very different due to factors such as bending of the fibres in the motion the worm makes while spinning the cocoon. Other observations on *B. mori* report different tensile properties in different parts of the cocoon [17,18].

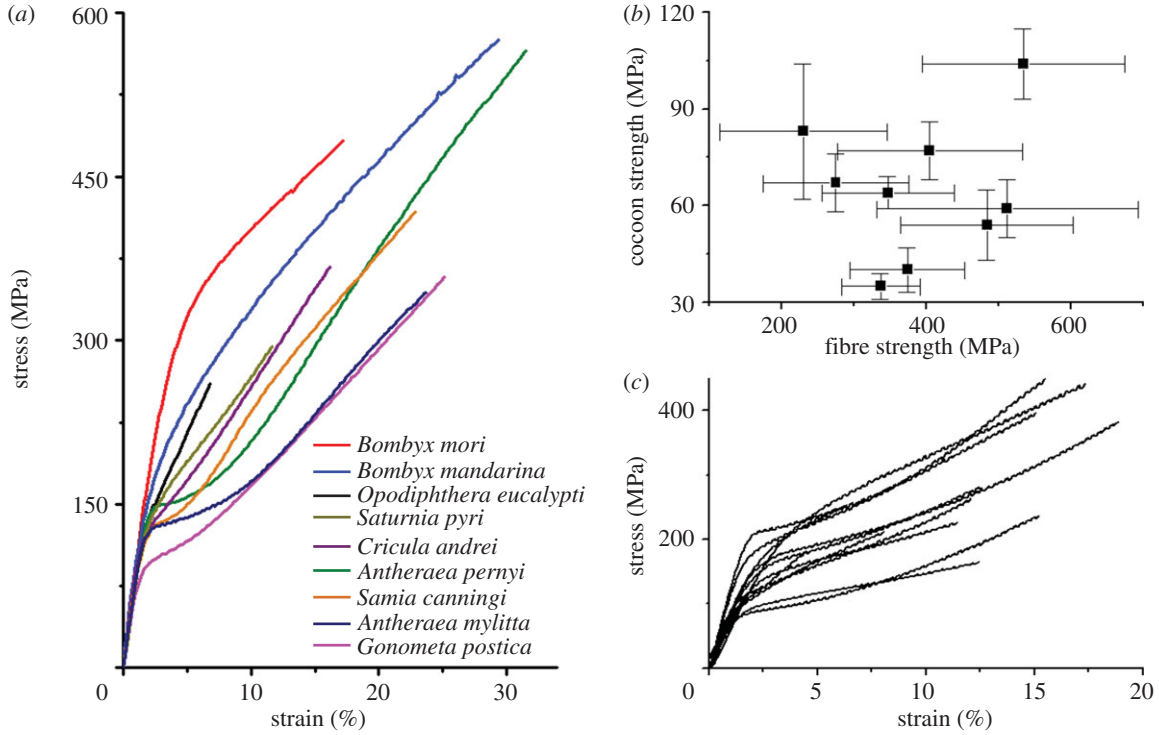

Figure 3. Tensile behaviour of silk fibres. (*a*) Average stress versus strain curves of different silk fibres. (*b*) No correlation between cocoon and fibre strength, $R^2 = 0.2$. (*c*) Variation in fibre properties, (*Saturnia pyri* fibre).

We will see later that the main fibre parameters that enter models for cocoon properties are low strain elastic modulus and activation strain to break. Here, we suggest that all the different fibres tested have essentially the same effective properties for cocoon fabrication.

It has amply been demonstrated already that the degumming process can have considerable effects on silk fibre properties [19,20] relieving us from demonstrating the mechanical behaviour of fibres degummed with different agents. The harsh degumming procedures required for highly bonded cocoons can severely degrade the structure and properties of the fibres themselves [19]. At the simplest level, non-degummed fibres in figure 3 would have larger cross-sectional areas than degummed owing to the weaker sericin layer, leading to a lower strength and modulus values compared with the literature.

2.3. Tensile properties

All of our cocoons have a similar general form to their tensile stress–strain deformation profile in the plane of the cocoon wall. The stress rises with strain to a maximum value and the gradient of this curve can change once or twice through apparent yield points until stress falls relatively rapidly after the maximum. Looking at all the stress–strain profiles in figure 3, we see that these yield points are quite consistent in strain 12–18% across almost all the cocoons, but their combinations and permutations in stress create an interesting diversity.

We categorized the cocoons into four types based on their tensile behaviour and their microstructure (figure 4). 'Lattice' cocoons (figure 4*a*) have only a loose scaffold structure made up of a few fused fibre bundles supporting the cocoon frame with large pores. The fibres sustain the load when the cocoon is stretched and the stress drops rapidly when the fibre bundles break. 'Weak' cocoons (figure 4*b*) have high porosity and weak interlayer bonding. The inter-fibre bonding breaks gradually with increasing strain, and the stress peaks at 15–20% strain and drops gradually when the unbonded fibres unravel from the non-woven structure. 'Brittle' cocoons (figure 4*c*) usually have a low porosity and strong interlayer bonding or a single layer structure. A crack starts from the sericin-binding matrix and grows perpendicular to the tensile load, leading to fibre breakage and a dramatic stress drop at 15–25% strain. 'Tough' cocoons (figure 4*d*) can be grouped into a fourth type, in which the cocoons have medium porosity and interlayer bonding. These cocoons have the most complex stress–strain profiles, with multiple yield points below 20 per cent strain and then a rapid failure in the range 40–60% strain, where the sericin binder matrix fragments and the fibres pull apart as a global unravelling.

In previous work [8,21], we observed that some of the more obviously non-woven structured cocoons follow the open cell foam model developed by Zhu *et al.* [22] whereby the elastic modulus of the cocoon is controlled by density (governed by the porosity of the cocoon and packing density of the fibres) and the elastic modulus of the fibres through a process of bending of the fibres between bonding junctions. As the fibres have very similar modulus values and density from our experimental results, the cocoons simply follow a Gibson–Ashby type [23] of relation very approximately in density squared, which is plotted in

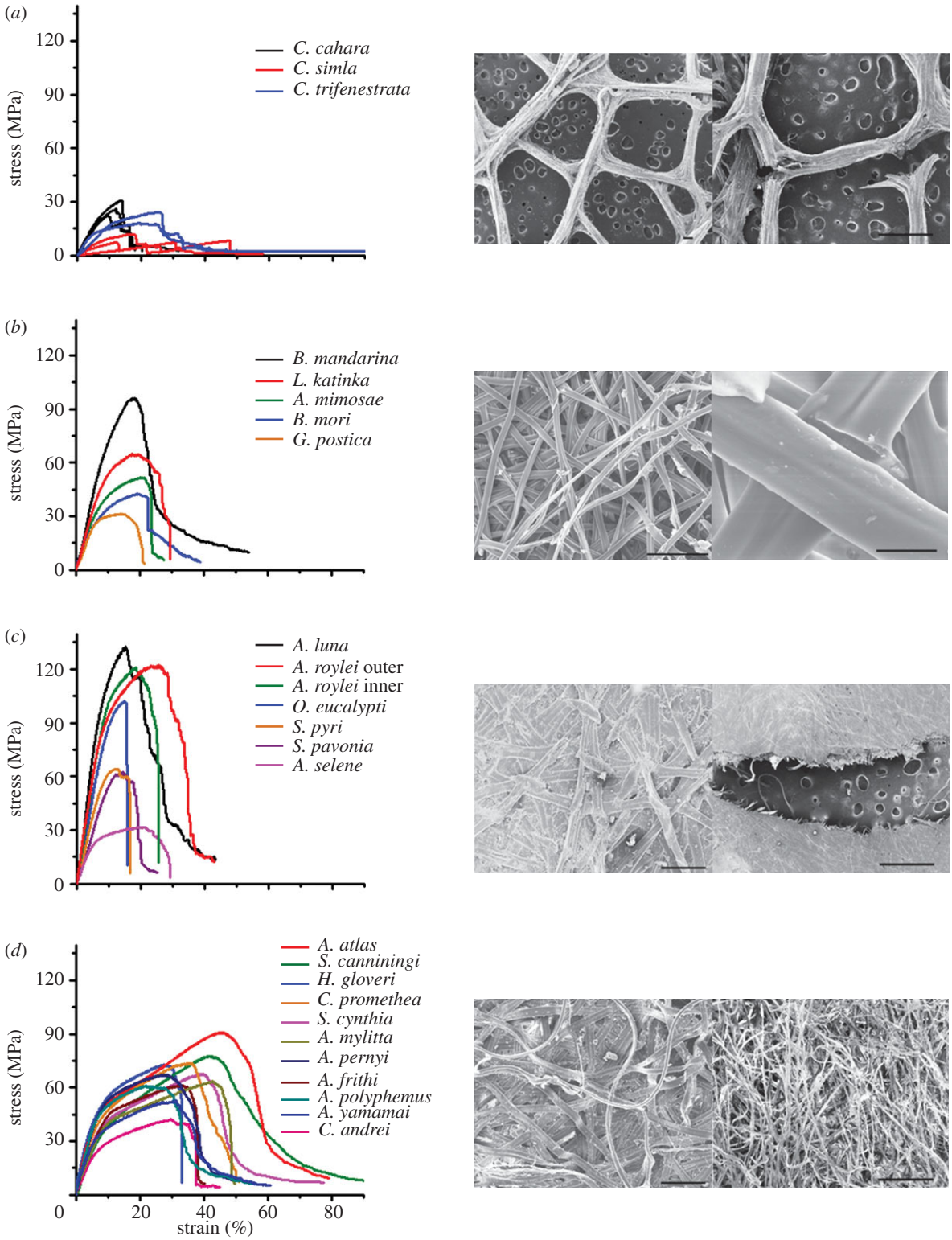

Figure 4. Tensile behaviour of silkworm cocoons. (*a*) 'Lattice' cocoons. SEM pictures of *C. simla*. Left: surface structure, scale bar: 200 µm. Right: breaking mechanism, scale bar: 1 mm. (*b*) 'Weak' cocoons. SEM pictures of *B. mori*. Left: surface structure, scale bar: 200 µm. Right: breaking mechanism, scale bar: 20 µm. (*c*) 'Brittle' cocoons. SEM pictures of *S. pavonia*. Left: surface structure, scale bar: 200 µm. Right: breaking mechanism, scale bar: 1 mm. (*d*) 'Tough' cocoons. SEM pictures of *S. cynthia*. Left: Surface structure, scale bar: 200 µm. Right: breaking mechanism, scale bar: 1 mm.

figure 5 to illustrate the general overall trend in our dataset. However, we emphasize that this is only a trend, and that the many variables in cocoon morphology would not be expected to give a simple relation across the whole dataset.

We have developed a quantitative model to describe the damage mechanism for a very limited group of representative cocoons from three species: *B. mori, A. pernyi* and *O. eucalypti* [8,21]. These cocoons were selected because they display three distinct levels of

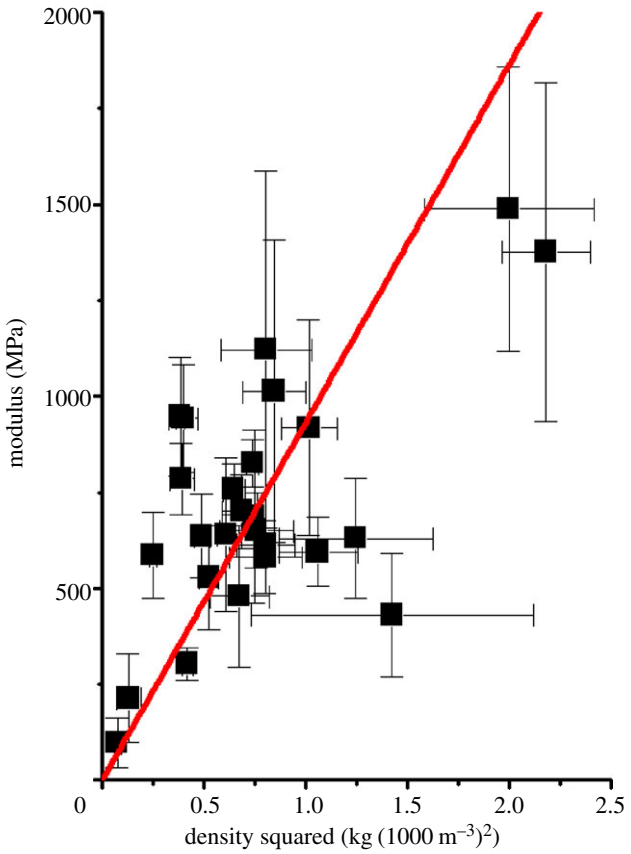

Figure 5. Tensile behaviour of silkworm cocoons: modulus versus density squared $R^2 = 0.41862$. (Online version in colour.)

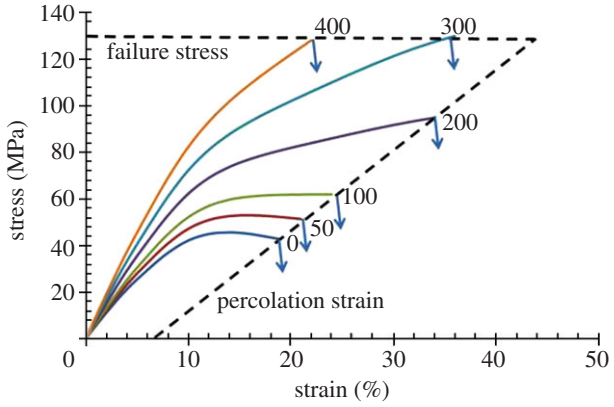

Figure 6. Model for nonwoven cocoons with different amounts of interfibre bonding, where the cocoon strength is bounded by dashed lines for percolation strain and the strength of the sericin binder. (Online version in colour.)

porosity from the sericin distribution between the fibres in SEM micrographs. This selection of cocoons gave clear indications of a general mechanism for cocoon tensile properties, where the contributions of sericin binder, fibre and the connectivity level of binding between fibres could be quantified by a self-consistent set of activation parameters in strain to describe the gradual loss of structural interfibre bonding connectivity in the composite, which manifests itself as a gradually decreasing modulus up to a percolation threshold of connectivity for rapid failure, where half of the bonding connectivity is lost under strain. The model is illustrated in figure 6, which shows the stress–strain profile of cocoons with different extents of inter-fibre bonding, which is quantified by the numerical labels on the curves, representing the single variable parameter of inter-fibre bonding contribution to the cocoon modulus in the model.

The data displayed in figure 6 demonstrate the limits of cocoon strength, as the dashed line envelope bounded by the percolation strain for loss of bonding connectivity and the upper stress bound of the individual strength of the sericin binder. Here, we define percolation strain as the strain at which the silk network in cocoons loses connections and behaves like an unconnected fibre arrangement. While the model is very simple and does not consider detailed features of cocoon morphology, comparison with experimental observations in figure 3 shows that it captures the key features of most of the cocoon stress–strain profiles. All the samples have a gradual reduction of the modulus as connectivity is lost and a percolation threshold follows. Two critical strains, 6 and 16 per cent, are observed in all of the curves, which represent sericin and fibre failure individually according to the model.

The 'tough' cocoons (figure 4*d*) would have a third higher activation strain at around 60 per cent associated with the interfibre bonding connectivity, depending on their individual morphologies. However, this activation strain is not usually observed directly as a yield point because global failure usually precedes it. The 'brittle' cocoons (figure 4*c*) with low porosity and a high bonding area, in contrast, usually fail by crack propagation through the compact combination of fibres and matrix, and their strength often has an upper limit of about 130 MPa, which is the strength of the sericin matrix. We also note that fibres break during the catastrophic failure of the material at their model characteristic failure strain of about 16 per cent. On the other hand, the 'weak' cocoons (figure 4*b*) have a high porosity and the structure fails when about half of the bonding between fibres breaks, and the unbonded fibres are pulled out with hardly any fibre breaks, which is represented as a long tail in the stress–strain curves.

Future work will add further refinements to the model and attempt to emulate the properties of all types of cocoon.

2.4. Compressive properties

All cocoons under compressive stress perpendicular to the plane of the walls have consistent stress-density behaviour. Due to their initial loose structure at the beginning of compression up to about 0.5 MPa, the stress increases slowly with a relatively large increase in density.

The compressive behaviour of cocoons is classified into three categories (figure 7). Of main interest here are cocoons with a porous three-dimensional nonwoven structure, shown as the central block of stress–density curves in figure 7*b* with structures of a form shown in the micrograph. Either side of this central block, the low-density 'lattice' cocoons (figure 7*a*) and the high-density 'brittle' cocoons (figure 7*c*) are difficult

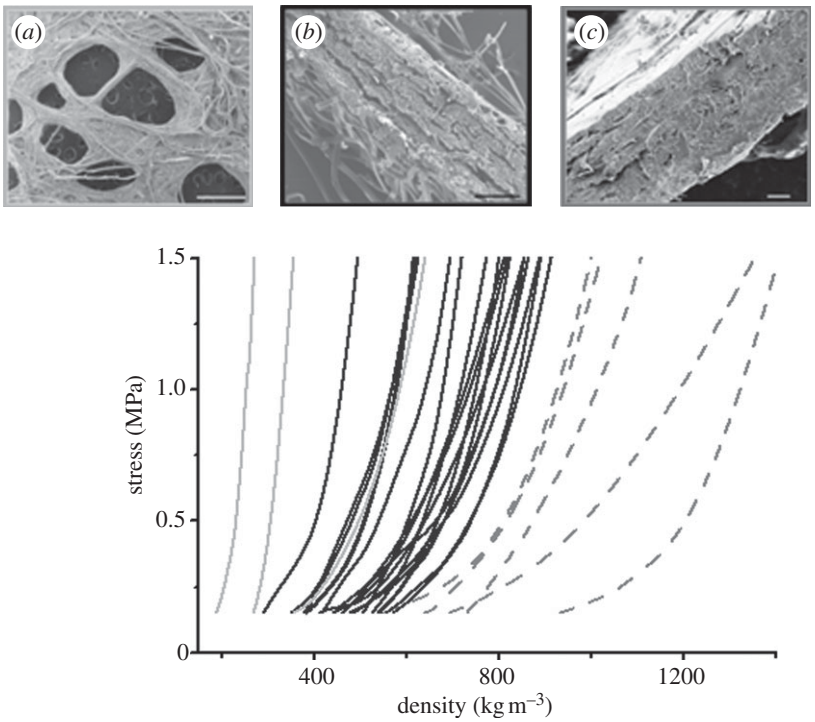

Figure 7. Compressive behaviour of silkworm cocoons. (*a*) Cocoons with lattice structure, *C. trifenestrata* (light grey lines); (*b*) cocoons with weak interlayer bonding, *B. mori* (solid lines); (*c*) cocoons with strong interlayer bonding or single layer, *O. eucalypti* (dark grey dashed lines). Scale bar (*a*–*c*): 200 µm.

to compress above the 0.5 MPa level, since compression is against a solid fibre or composite material, with no effective pores to compact in the compression axis.

Between the lower and upper ranges of loose fibre and solid material compaction, respectively, the compressive behaviour of non-woven cocoons is found to follow the mat consolidation model developed by Zhou *et al.* [24] for wood composites. This model treats a composite mat structure as a system of bending beams, in a similar fashion to the open cell foam model used for tensile deformation, but with a different geometry of forces applied to beam segments between the bonded contact points. The number of contact points and the length of the bending segments of fibre decrease with increasing density, thereby increasing the compressive stress in a highly nonlinear manner. The model predicts that compressive pressure, P, should increase in a power 5 of density with a form

$$P = \frac{K\ E_s}{\rho_s}(\rho_m^5 - \rho_o^5), \tag{2.1}$$

where E_s and ρ_s are the modulus and density of the fibres, respectively, ρ_m is the density of the mat, ρ_o is the initial mat density and K is a dimensionless proportionality constant.

In the case of our non-woven cocoons, the power of 5 for pressure on density is found to be a characteristic of the consolidation of the non-woven structure, as shown in figure 8, where cocoons from the central block of figure 7*b* are plotted in a log–log pressure–density graph against a reference curve (red) with a power 5 in density. Thus, the model developed for wood-based composites appears to work well for non-woven cocoon structures, and suggests that the dominant mechanism for compaction resistance is fibre bending.

2.5. Gas diffusion

We can suppose that gas and water vapour diffusion must play an important role in the development of pupae in cocoons and perhaps control the barrier characteristic of the cocoon to threats such as bacteria [7]. However, at the moment we have no quantitative information about the biological role of diffusion. Here, we report our observations on gas diffusion through cocoons as a physical process and make an initial attempt to demonstrate how the structural and morphological features of different cocoons affect diffusion properties.

As detailed in the experimental section, we quantified the rate of gas (diethyl ether) through a cocoon by measuring the weight loss of liquid by evaporation and diffusion through a section of cocoon mounted on the end of an otherwise impermeable tube. We found that the mass loss was almost linear with time, so to compare the different cocoons in each test, we classified the absolute diffusion rate results in terms of cocoon morphology into four groups as shown in the micrographs at the bottom of figure 9 and grouped in the associated bar chart by colour as a guide to the main contributory features that controlled diffusion. Clearly, all the cocoons reduce the speed of gas diffusion with cocoon thickness, porosity and calcium oxalate crystals affecting rate of diffusion. *Actias selene, A. luna* and *O. eucalypti* cocoons all have low porosity which allow them to conserve the gas, and hence the cocoons have lowest gas diffusion

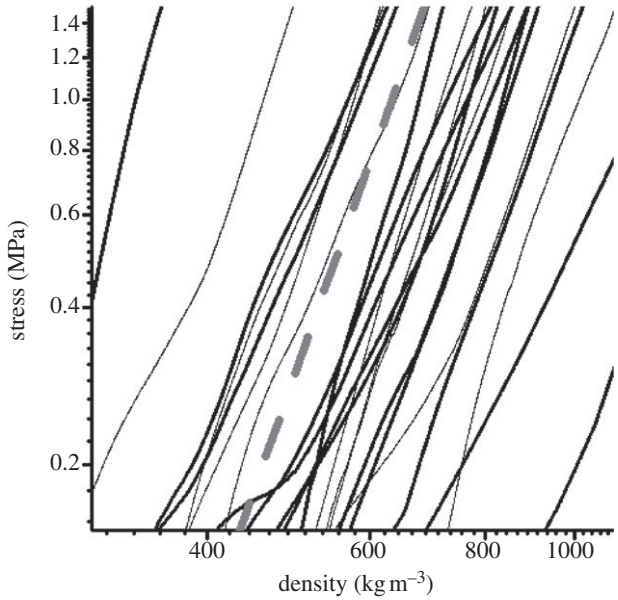

Figure 8. Compressive behaviour of silkworm cocoons: log–log stress versus density. The dashed line is a straight line of 10 to the power of 5 to illustrate the model relation of equation (2.1).

rate among the specimens tested. Cocoons with calcium oxalate crystals on the surface also have lower gas diffusion rate, e.g. those produced by *Hyalophora gloveri, Antheraea frithi, S. pyri, Samia canningi and Gonometa postica*, etc. This may be due to the dense crystals filling the pores. *Actias atlas, B. mori* and *C. cachara* cocoons have a high-porosity structure, leading to high gas diffusion rate.

Without making a detailed analysis of the diffusion results at this stage in our work, figure 10 shows that density of the cocoons has a sensible correlation with gas diffusion rate, i.e. a higher density slows down the permeation rate of gas (diethyl ether) through the cocoon.

3. CONCLUSIONS

We present our observations and measurements on 25 diverse types of cocoon in a first attempt to correlate physical properties with the structure and morphology of the cocoons, which appears to be more important than the differences in the properties of the silk fibres themselves. We find that the inter-fiber variability of properties is similar to that of an individual fibre type, and that the important fibre properties of low strain modulus and strain to failure for cocoon properties are similar for all the fibre types tested.

We tested tensile and compressive mechanical properties and gas permeation of the cocoon walls, and in each case identify mechanisms or models that relate these properties to cocoon structure. For tensile properties in the plane of the cocoon walls, we identify four different types of cocoon behaviour. However, the same generic mechanisms are seen in all types of cocoon. The connectivity of inter-fiber bonding plays a dominant role in stress–strain properties, and failure conditions are determined either by the percolation

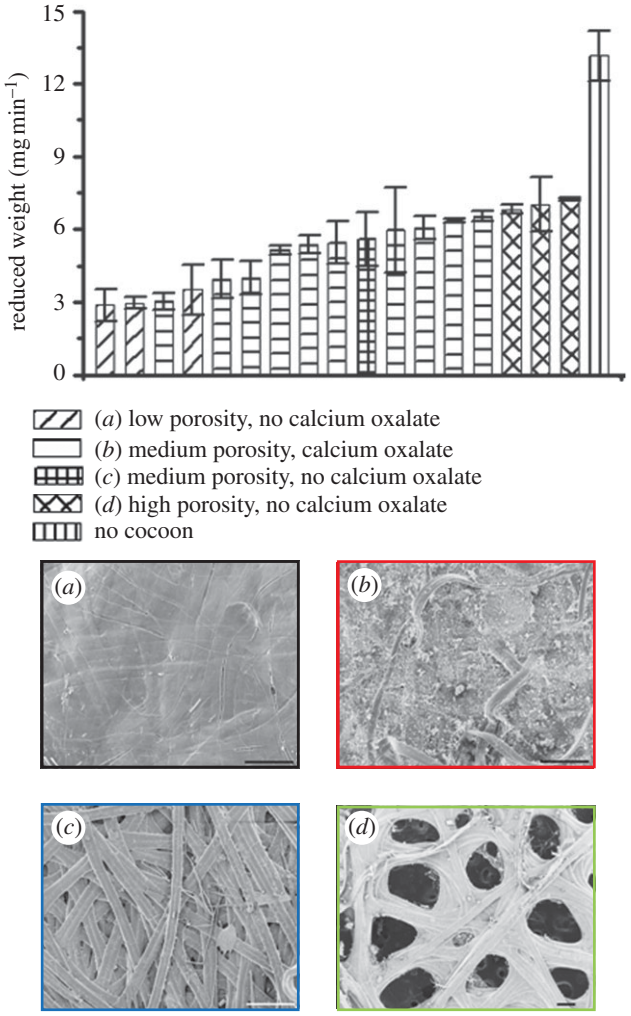

Figure 9. Gas diffusability (diethyl ether) of silkworm cocoons. Top: comparison of diffusability speed of different cocoons. From left to right: *A. luna*, *O. eucalypti*, *S. pyri*, *A. selene*, *H. gloveri*, *A. frithi*, *S. canningi*, *A. mylitta*, *A. pernyi*, *L. katinka*, *A. polyphemus*, *A. yamamai*, *G. postica*, *A. atlas*, *B. mori*, *C. cachara*, *A. roylei*, no cocoon. Bottom: morphologies of example cocoons. (*a*) Cocoons with low porosity and no calcium oxalate: *O. eucalypti*. (*b*) Cocoons with medium porosity and calcium oxalate: *A. frithi*. (*c*) Cocoons with medium porosity and no calcium oxalate: *L. katinka*. (*d*) Cocoons with high porosity and no calcium oxalate: *C. cachara*. Scale bar (*a–d*): 200 µm. (Online version in colour.)

strain for loss of bonding connectivity or sericin binder strength, whichever is the lower.

Compressive properties normal to the plane of the cocoon walls are dominated by density, and a model previously derived for wood mats seems to be applicable and explain the stress–strain behaviour as a power 5 dependence of stress upon density under load. Gas diffusion through the cocoon walls is controlled by the combination of thickness and density, and contributions due to features such as calcium oxalate crystals are identified.

4. EXPERIMENTAL SECTION

4.1. Materials collection

Bombyx mori silkworms were raised in a laboratory ($23 \pm 2^{\circ}$C, 60% relative humidity) and fed with

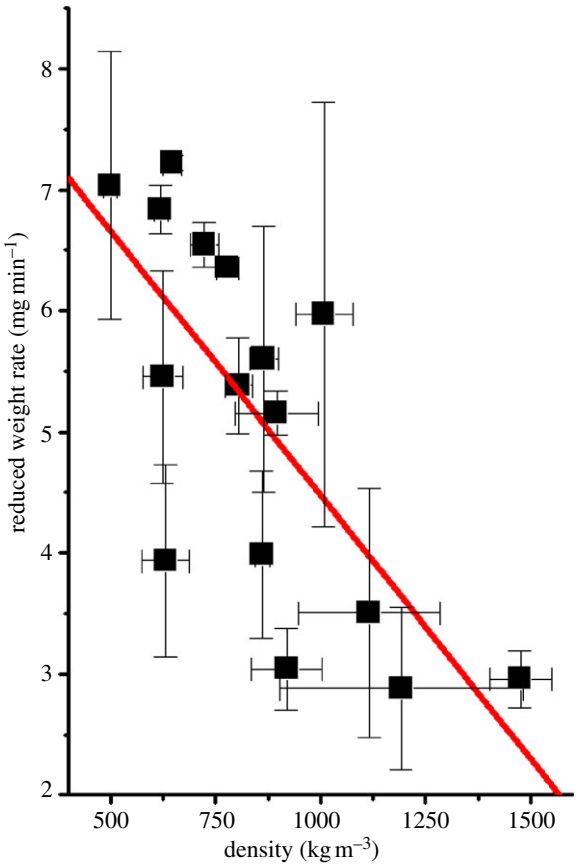

Figure 10. Gas diffusion (diethyl ether) rate of silkworm cocoons plotted as the rate of normalized mass loss against the density. $R^2 = 0.51802$. (Online version in colour.)

mulberry leaves until they spun cocoons in a dark environment. *Bombyx mandarina* and *G. postica* cocoons were collected separately in Anhui, China and Nairobi, Kenya. All the other cocoons were purchased from Worldwide Butterflies, UK. Cocoons were examined after the pupae had left them by tunnelling through one end. The selection criterion of cocoons investigated in this section is the availability of the material.

4.2. Scanning electron microscope observation

Cocoons were hole punched at the middle section to make samples with a diameter of 3.5 mm which were glued onto a superconducting tape and sputter coated in Quorum Technologies SC 7620. The coated samples were transferred into the Jeol Neoscope JCM-5000 SEM for observation at 15 V. After mechanical testing, the samples were collected for SEM with the same procedure.

4.3. Tensile tests of cocoons

Strips of cocoons in the direction of the long axis were cut for samples with a width of 5 mm and length of 15 mm. Tensile tests were carried out using Instron 5542 with a speed of 2 mm min^{-1} and 5 mm gauge length. The stress was calculated from the nominated thickness of the samples. Three samples from each cocoon species were tested.

4.4. Fibre testing

In the textile industry, *B. mori* cocoons are submerged in water and detergents are added to remove the sericin glue from the cocoon to unravel the fibres. It has been found that the degumming had quantitative effects on the mechanical properties of the fibres [20,25]. In order to understand the original contribution of fibres in the cocoon, we investigated the tensile behaviour of composite fibres covered with sericin rather than industrial degummed fibres, and hence a destoning method was used for unravelling the cocoons. This method uses ethylenediaminetetraacetic acid (EDTA) and has been found to succeed in unravelling the cocoon and causes less damage to both the sericin and the fibres [26]. EDTA powders from Fisher Scientific were dissolved to make a 1 mol l^{-1} solution, and sodium hydroxide pellets (Sigma) were dissolved in the liquid to get a pH value of 7. The solution was stirred constantly and heated to a temperature of 60°C during the dissolving process. When the solutes were fully dissolved, each cocoon was degummed by treatment with a 1 l solution in a vacuum oven at 40°C for 48 h. The degummed cocoons were washed thoroughly in clean water and then dried in air. Fibres were collected by reeling at a speed of 80 cm min^{-1}. For those cocoons which could not be reeled by machinenary even after degumming, the fibres were carefully collected by hand. Fibre samples were mounted on paper frames with 10 mm gauge length and tested in Instron 5542 at 0.18 s^{-1} strain rate. Twenty samples from three cocoons in each species were chosen for tests.

4.5. Compression tests of the cocoons

A TA Instruments Q800 Dynamic Mechanical Thermal Analyser (DMTA) in compression mode was used to test the compressive behaviour of the cocoons. Cocoons were cut into circular samples with a diameter of 3.5 mm and weighed before tests. A metal plate applied a compressive force on the sample at a speed of 3 N min^{-1}. The tests automatically stopped when the compressive stress reached 1.5 MPa. The data of force versus distance of the plate were recorded for analysis. Three samples from each cocoon species were tested.

As the cocoon wall has a porous structure, its thickness varies according to the force applied on it. This raises the question of how to define the thickness for calculating the strength of the materials. In this paper, the nominated thicknesses of the cocoons were defined at 1.5 MPa compressive stress. The density of the cocoons was then calculated from this nominated thickness and the weight of the samples.

4.6. Gas diffusion test

An airtight diffusion cell made from a modified screw-cap centrifuge tube was used to hold the circular cocoon sample with a diameter of 12 mm. The diffusion cell was filled with 0.35 ml diethyl ether covered with the sample, and placed on an electric balance to measure the reducing weight with the evaporation of the ether as a function of time using a connected computer. Seventeen species of cocoons were measured

with three samples each. The diffusion of ether with no cocoon in the cell was also recorded for comparison. The test was carried out at 22°C and 51 per cent RH (see the electronic supplementary material).

We are grateful to Ms Juan Guan and Dr Chris Holland for working on compressive tests and to Mr Tom Gheysens, Dr Cedric Dicko and Mr Bjourn Greving for developing cocoon destoning, gas diffusion and fibre diameter measurement method. Mr Xiafu Shi also kindly helps with the cocoon photographs. We particularly thank Prof. Richard S. Peigler for checking the silkmoth species spelling. This project was funded by AFSOR (F49620-03-1-0111) and ERC (SP2-GA-2008-233409).

REFERENCES

1 Porter, D. & Vollrath, F. 2009 Silk as a biomimetic ideal for structural polymers. *Adv. Mater.* **21**, 487–492. (doi:10.1002/adma.200801332)
2 Danks, H. V. 2004 The roles of insect cocoons in cold conditions. *Eur. J. Entomol.* **101**, 433–437.
3 Tuskes, P. M. P. & Paul, P. M. 1996 *The wild silk moths of North America: a natural history of the Saturniidae of the United States and Canada*. Ithaca, NY: Cornell University Press.
4 Zhao, H.-P., Feng, X.-Q., Yu, S.-W., Cui, W.-Z. & Zou, F.-Z. 2005 Mechanical properties of silkworm cocoons. *Polymer* **46**, 9192–9201. (doi:10.1016/j.polymer.2005.07.004)
5 Zhao, H.-P., Feng, X.-Q., Cui, W.-Z. & Zou, F.-Z. 2007 Mechanical properties of silkworm cocoon pelades. *Eng. Frac. Mech.* **74**, 1953–1962. (doi:10.1016/j.engfracmech.2006.06.010)
6 Reddy, N. & Yang, Y. 2010 Structure and properties of cocoons and silk fibers produced by *Hyalophora cecropia*. *J. Mater. Sci.* **45**, 4414–4421. (doi:10.1007/s10853-010-4523-3)
7 Blossman-Myer, B. & Burggren, W. W. 2010 The silk cocoon of the silkworm, *Bombyx mori*: macro structure and its influence on transmural diffusion of oxygen and water vapor. *Comp. Biochem. Physiol.—Part A Mol. Integr. Physiol.* **155**, 259–263. (doi:10.1016/j.cbpa.2009.11.007)
8 Chen, F., Porter, D. & Vollrath, F. 2010 Silkworm cocoons inspire models for random fiber and particulate composites. *Phys. Rev.* **E82**, 041911–041917. (doi:10.1103/PhysRevE.82.041911)
9 I'Anson, S. J. & Sampson, W. W. 2007 Competing Weibull and stress-transfer influences on the specific tensile strength of a bonded fibrous network. *Compos. Sci. Technol.* **67**, 1650. (doi:10.1016/j.compscitech.2006.07.002)
10 Eichhorn, S. J. & Sampson, W. W. 2009 Relationships between specific surface area and pore size in electrospun polymer fibre networks. *J. R. Soc. Interface* **7**, 641–649. (doi:10.1098/rsif.2009.0374)
11 Hoseini, M., Bindiganavile, V. & Banthia, N. 2009 The effect of mechanical stress on permeability of concrete: a review. *Cement Concrete Composites* **31**, 213–220. (doi:10.1016/j.cemconcomp.2009.02.003)
12 Kothari, V. K. & Das, A. 1992 Compressional behaviour of nonwoven geotextiles. *Geotext. Geomembranes* **11**, 235–253. (doi:10.1016/0266-1144(92)90002-R)
13 Rawal, A. & Anandjiwala, R. 2007 Comparative study between needlepunched nonwoven geotextile structures made from flax and polyester fibres. *Geotext. Geomembranes* **25**, 61–65. (doi:10.1016/j.geotexmem.2006.08.001)
14 Correia, N. d. S. & Bueno, B. d. S. 2011 Effect of bituminous impregnation on nonwoven geotextiles tensile and permeability properties. *Geotext. Geomembranes* **29**, 92–101. (doi:10.1016/j.geotexmem.2010.10.004)
15 Chen, F., Porter, D. & Vollrath, F. 2011 Silk cocoon (*Bombyx mori*): Multi-layer structure and mechanical properties. *Mater. Sci. Eng. C-Biomimetic and Supramolecular Systems*, Submitted.
16 Freddi, G., Gotoh, Y., Mori, T., Tsutsui, I. & Tsukada, M. 1994 Chemical structure and physical properties of *Antheraea assama* silk. *J. Appl. Polym. Sci.* **52**, 775–781. (doi:10.1002/app.1994.070520608)
17 Zhao, H.-P., Feng, X.-Q. & Shi, H.-J. 2007 Variability in mechanical properties of *Bombyx mori* silk. *Mater. Sci. Eng. C.* **27**, 675–683. (doi:10.1016/j.msec.2006.06.031)
18 Perez-Rigueiro, J., Viney, C., Llorca, J. & Elices, M. 1998 Silkworm silk as an engineering material. *J. Appl. Polym. Sci.* **70**, 2439–2447. (doi:10.1002/(SICI)1097-4628(19981219)70:12<2439::AID-APP16>3.0.CO;2-J)
19 Jiang, P., Liu, H. F., Wang, C. H., Wu, L. Z., Huang, J. G. & Guo, C. 2006 Tensile behavior and morphology of differently degummed silkworm (*Bombyx mori*) cocoon silk fibres. *Mater. Lett.* **60**, 919–925. (doi:10.1016/j.matlet.2005.10.056)
20 Perez-Rigueiro, J., Elices, M., Llorca, J. & Viney, C. 2002 Effect of degumming on the tensile properties of silkworm (*Bombyx mori*) silk fiber. *J. Appl. Polym. Sci.* **84**, 1431–1437. (doi:10.1002/app.10366)
21 Chen, F., Porter, D. & Vollrath, F. 2010 A nonwoven composite model based on silkworm cocoon (*Bombyx mori*). *J. Mater. Sci. Eng.* **4**, 28–33.
22 Zhu, H. X. 1997 Analysis of the elastic properties of open-cell foams with tetrakaidecahedral cells. *J. Mech. Phys. Solids* **45**, 319. (doi:10.1016/S0022-5096(96)00090-7)
23 Gibson, L. J. & Ashby, M. F. 1982 The mechanics of three-dimensional cellular materials. *Proc. R. Soc. Lond. A Math. Phys. Sci.* **382**, 43–59. (doi:10.1098/rspa.1982.0088)
24 Zhou, C., Dai, C. & Smith, G. D. 2008 A generalized mat consolidation model for wood composites. *Holzforschung* **62**, 201–208. (doi:10.1515/hf.2008.053)
25 Poza, P., Perez-Rigueiro, J., Elices, M. & Llorca, J. 2002 Fractographic analysis of silkworm and spider silk. *Eng. Frac. Mech.* **69**, 1035–1048. (doi:10.1016/S0013-7944(01)00120-5)
26 Gheysens, T., Collins, A., Raina, S., Vollrath, F. & Knight, D. P. 2011 Demineralization enables reeling of wild silkmoth cocoons. *Biomacromolecules*. 12, 2257–2266. (doi:10.1021/bm2003362)